Pharm Res (2012) 29:121–133
DOI 10.1007/s11095-011-0519-1

RESEARCH PAPER

Photolysis of Recombinant Human Insulin in the Solid State: Formation of a Dithiohemiacetal Product at the C-Terminal Disulfide Bond

Olivier Mozziconacci • Jessica Haywood • Eric M. Gorman • Eric Munson • Christian Schöneich

Received: 29 April 2011 / Accepted: 17 June 2011 / Published online: 12 July 2011

ABSTRACT

Purpose Exposure of protein pharmaceuticals to light can result in chemical and physical modifications, potentially leading to loss of potency, aggregation, and/or immunogenicity. To correlate these potential consequences with molecular changes, the nature of photoproducts and their mechanisms of formation must be characterized. The present study focuses on the photochemical degradation of insulin in the solid state.

Methods Solid insulin was characterized by solid-state NMR, polarized optical microscopy and scanning electron microscopy; various insulin preparations were exposed to UV light prior to product analysis by mass spectrometry.

Results UV-exposure of solid human insulin results in photodissociation of the C-terminal intrachain disulfide bond, leading to formation of a $CysS^{\bullet}$ thiyl radical pair which ultimately disproportionates into thiol and thioaldehyde species. The high reactivity of the thioaldehyde and proximity to the thiol allow the formation of a dithiohemiacetal structure. Dithiohemiacetal is formed during the UV-exposure of both crystalline and amorphous insulin.

Conclusions Dithiohemiacetals represent novel structures generated through the photochemical modification of disulfide bonds. This is the first time that such structure is identified during the photolysis of a protein in the solid state.

KEY WORDS amorphous · crystal structure · cysteine · disulfide · mass spectrometry · photolysis · solid state · stability · thiyl radical · UV irradiation

Electronic Supplementary Material The online version of this article (doi:10.1007/s11095-011-0519-1) contains supplementary material, which is available to authorized users.

O. Mozziconacci · J. Haywood · E. M. Gorman · E. Munson · C. Schöneich (✉)
Department of Pharmaceutical Chemistry University of Kansas
2095 Constant Avenue, Lawrence, Kansas 66047, USA
e-mail: schoneic@ku.edu

Present Address:
E. Munson
Department of Pharmaceutical Sciences
University of Kentucky
Lexington, Kentucky 40506, USA

INTRODUCTION

Proteins represent a rapidly growing class of therapeutics developed by the biotechnology industry (1). Proteins are sensitive to a large array of physical and chemical modifications caused by pH, adjuvants, temperature, sterilization (2,3), and methods of viral decontamination (4,5), and it is mandatory to evaluate the nature of degradation products and degradation mechanisms for product characterization and the rational development of stable formulations (6). The exposure to light has been identified as a major problem for protein stability (6). In proteins, light is predominantly absorbed by tryptophan, tyrosine, cystine (Cys disulfide bond) and phenylalanine. Tryptophan and tyrosine photolysis can result in photoionization yielding an intermediary aromatic radical cation and an electron. The latter can react with a disulfide, resulting in the formation of a thiyl radical and thiolate (7,8); depending on the aromatic amino acid, the ensuing aromatic radical cation can react via one-electron transfer (9–14), deprotonation (15,16), the addition of water and/or recombination with the thiyl radical (17). A number of photolytically sensitive protein pharmaceuticals have been identified (6). Well-established photoproducts from Trp, Tyr, and cystine include N-formylkynurenine, oxoindole,

dityrosine, sulfonic and sulfinic acid. The disulfide bond is sensitive to light-induced degradation, where recent studies with model peptide have indicated the formation of a series of novel photoproducts such as dithiohemiacetals, and thioethers (18–21). Additionally, in a previous publication, we investigated in particular the mechanisms of photodegradation of human insulin in solution through the formation of S-centered radicals, where evidence for chemical cross-linking between the A- and B-chain was obtained, together with significant extent of covalent H/D exchange when experiments were carried out in D_2O (22). Evidence for dithiohemiacetal formation was presented also for the photoirradiation of an immunoglobulin, IgG1, in solution (18). Earlier studies on the degradation of human growth hormone (hGH) had documented the formation of a thioether variant and a reduced affinity of such thioether variant of hGH to its respective receptors (23,24). The important question is whether such products are also formed during photoirradiation of protein solids. Some common degradation products of protein solids have been documented (25–28). However, the photodegradation of solid proteins has only been studied in a few cases (29,30). It was pointed out that, especially for 253.7 nm irradiation, protein damage can be associated with disulfide degradation, in part due to the difference in quantum yields for disulfide photochemistry compared to the photochemistry of the aromatic amino acids (30). We report here that the UV-exposure of solid human insulin results in the rearrangement of the disulfide bond between Cys[A20] and Cys[B19] into a dithiohemiacetal. Because it is known that the degradation of crystalline and amorphous forms of solid proteins may differ (31), we have characterized the physical form of the solid human insulin prior to photoirradiation.

MATERIALS AND METHODS

Materials

Human insulin (Fig. 1) was purchased from Roche Applied Science (Indianapolis, IN) and from Millipore (Billerica, MA). Bovine insulin was purchased from Sigma-Aldrich (St Louis, MO); all insulin samples were used without further purification. Ammonium bicarbonate (NH_4HCO_3), N-ethylmaleimide (NEM), dithiothreitol (DTT), sodium dodecyl sulfate (SDS), 4-(2-pyridylazo)-resorcinol (PAR), diethylmaleate (DEM), glutaraldehyde, isoamyl acetate, and hexamethyldisilazane were supplied by Sigma (St. Louis, MO) at the highest degree of purity. The sequencing grade Glu-C endoproteinase was supplied by Roche (Nutley, NJ). Deuterium oxide was supplied by Cambridge Isotope Laboratories, Inc. (Andover, MA) at 99.9% purity.

Analysis of the Physical Form of Insulin

Our photochemical experiments concerned the UV exposure of solid human insulin. However, in order to evaluate the physical form of insulin (crystalline or amorphous, respectively), we prepared reference samples of crystalline and amorphous bovine insulin according to published procedures (32,33).

Preparation of Crystalline and Amorphous Insulin Reference Samples

Crystalline bovine insulin was prepared by a previously reported method (32,33). Two solutions (Media A and B) were mixed to produce the crystallization media. Media A and B contained sufficient insulin so that when combined in a ratio of three parts A to one part B, the resulting crystallization media contained 1.7% (w/v) insulin, 0.155 mg/mL Zn^{2+} (either from the insulin itself or added as $ZnCl_2$), 7% (w/v) NaCl, 0.1 M sodium acetate, and the pH was adjusted to 5.45–5.55 with HCl and NaOH. Medium A contained $ZnCl_2$ (0.147 mg/mL) and 0.027 N HCl resulting in a pH of 2, while medium B contained sodium acetate (0.4 M), NaCl (0.28 g/mL), and 0.044 N NaOH resulting in a pH of 12. In all cases the appropriate amount of insulin was dissolved in medium A, to which either medium B or water was added to achieve the previously reported 3:1 dilution. In the case where medium B was used as the diluent, the pH was adjusted as

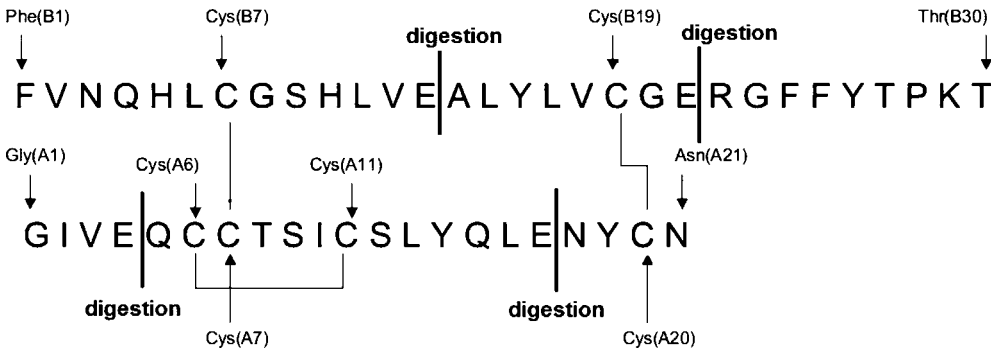

Fig. 1 Primary structure of human insulin with cleavage sites by Glu-C indicated.

previously reported (32,33) and the solution was stirred (200–300 rpm at 4°C) for 15 h to allow crystallization of any material that may have initially precipitated as amorphous insulin. The precipitate was then collected by vacuum filtration and allowed to dry under ambient conditions. To produce amorphous bovine insulin, the dilution was carried out with water in place of medium B, the pH was not adjusted, and the solution was placed in 20 mL glass scintillation vials (~10 mL of solution per vial) and flash frozen in liquid nitrogen for ~2-3 min. The vials of the frozen solution were then placed in a pre-cooled VirTis AdVantage lyophilizer (SP Scientific, NY), where they were maintained at −45°C for an additional 60 min and then underwent primary drying at −35°C for 24 h (vacuum of <100 mTorr) and secondary drying at 25°C for 5 h.

Sample Preparation for High-Performance Liquid Chromatography

The crystalline content of bovine and human insulin was quantified using the method reported in the 2005 U.S. Pharmacopeia National Formulary, with slight modifications. A buffered acetone solution was prepared according to the method of Bailey *et al.* (34). One mg of insulin was placed into a 1 mL microcentrifuge tube, and 100 µL of a 1:2 mixture of water and buffered acetone was added to the tube to extract any amorphous insulin. After 15 s of vortexing, the sample was immediately centrifuged at 13,000 rpm for 1 min in a microcentrifuge (SFR13K, Savant Instruments Inc., Holbrook, NY). The supernatant was decanted and the extraction repeated three times. Another 1 mg of insulin was placed into a microcentrifuge tube to be used as a control. Both samples were dissolved in 200 µL and 52 µL of HPLC solvents A and B, respectively. Solvent A was prepared by dissolving 28.4 g of anhydrous sodium sulfate in 1 L of milliQ water, to which 2.7 mL of phosphoric acid was added and the pH adjusted to 2.3 with ethanolamine. Solvent B consisted of 100% acetonitrile. Insulin was injected onto a 4.6×250 mm Symmetry C18 column (Waters Corp., Milford, MA) and eluted using an isocratic gradient (solvent A:solvent B, 74%:26%, v:v) at a flow rate of 1 mL/min.

The percentage of crystallinity was calculated as follows: % crystallinity = 100 × (peak area of the extracted sample) / (peak area of the control sample).

Determination of Zinc Content in Insulin

Zinc content in insulin samples was measured using the method developed by Crow *et al.* (35). Two mg of insulin were diluted into 1 mL of ammonium bicarbonate buffer at pH 7.8 in the presence of 1% SDS and 100 µM of PAR. The sample was incubated for 1 h at 80°C prior to measuring the absorbance at 500 nm. A calibration curve was obtained with different concentrations of $ZnCl_2$ (0–100 µM) in the presence of insulin.

^{13}C Solid-State NMR Analysis

^{13}C solid-state NMR analysis was performed to compare reference crystalline and amorphous bovine insulin and commercial human insulin with the solid material obtained after drying an aqueous solution originally containing 2.8 mg/mL of the commercial human insulin powder (see "Microcrystallization of Human Insulin"). Spectra were collected using a Tecmag Apollo spectrometer operating at a ^{1}H resonance frequency of 300 MHz using ramped amplitude cross-polarization (RAMP) (36), magic-angle spinning (MAS) (37), and SPINAL-64 decoupling (38). Samples were packed in 4 mm o.d. zirconia rotors using either Teflon or Torlon endcaps, spun at 8 kHz in a Chemagnetics™ Triple-Resonance APEX HXY CP/MAS NMR probe configured to run in double-resonance mode using the H and X channels, and fitted with a 4 mm spin module from Revolution NMR. All spectra are the sum of either 120,000 transients for bovine insulin or 48,000 transients for human insulin, collected using a 1.5 s pulse delay, a contact time of 2 ms, and a ^{1}H 90° pulse width of either 2.3 or 1.5 µs, respectively. The free induction decays consisted of 256 points with a dwell time of 33.3 µs. The spectra were externally referenced to tetramethylsilane using the methyl peak of 3-methylglutaric acid at 18.84 ppm (39).

Microcrystallization of Human Insulin

The microcrystals were prepared using a previously described method (40,41). Crystalline human insulin powders from Roche and Millipore, respectively, were completely dissolved in acetic acid (0.1 N) in the presence of zinc sulfate to reach a concentration of 1 mg/mL of insulin containing 0.4% (w/w) zinc ions. The pH of the solution was slightly increased to 6.0 by the addition of NaOH (1-10 N). The solutions were stirred for 30 min at room temperature, followed by stirring at 4°C overnight to allow the formation of microcrystals. The solutions were dried at room temperature.

Scanning Electron Microscopy Analysis

Scanning electron microscopy (SEM) was performed to compare the crystalline structures of the commercial human insulin from Roche and Millipore. SEM was also used to characterize the microcrystals prepared from the commercial insulins. Prior to the morphological analysis,

insulin was fixed with 2.5% glutaraldehyde in 0.1 M phosphate (pH 7) for 1 h at 4°C. Then, the samples were rinsed twice with PBS. The microcrystals were dehydrated in graded series of ethanol:water (70%, 80%, and 95% v:v). After centrifugation at 5,000 rpm for 2 min, the ethanol: water mixture was discarded and replaced by isoamyl acetate. After 10 min, the isoamyl acetate was discarded and replaced by hexamethyldisilazane. Under a gentle Ar-stream, the hexamethyldisilazane was removed and the insulin was sputter-coated with gold palladium before examination by SEM.

Preparation of Amorphous Human Insulin

Human insulin from Roche was freshly prepared at a concentration of 2.8 mg/mL in H_2O or D_2O, and 400 µL were placed into quartz tubes. The samples were dried under vacuum in a SpeedVac for 3 h. The amorphous nature was confirmed analytically by the method described in "Sample Preparation for High-Performance Liquid Chromatography."

UV-Irradiation

Quartz tubes containing insulin were Ar-saturated prior to UV-exposure. Four types of solids were photoirradiated: i) human insulin powder obtained from Roche, ii) human insulin solid obtained after drying a solution of insulin from Roche at a concentration of 2.8 mg/mL (see "Preparation of Amorphous Human Insulin"), iii) human insulin powder obtained from Millipore, iv) microcrystals from Millipore insulin prepared according to the protocol described in "Microcrystallization of Human Insulin." All samples were photoirradiated for up to 30 min at 253.7 nm with a handle lamp emitting at 253.7 nm (UVLMS-38 EL series 3UV lamp, UVP, Upland, CA; flux = 3.18×10^{-7} einstein s^{-1}; the flux of photons was measured by actinometry (42)).

Derivatization and Proteolytic Digestion of Photoirradiated Human Insulin

Derivatization

Stock solutions of NEM, DEM and DTT were freshly prepared at a concentration of 0.1 M each in MilliQ water. The thiol residues, generated during the UV-exposure of insulin, were derivatized by dilution of 100 µL of the irradiated sample in a solution containing 50 µL of NEM stock solution and 700 µL of buffer (50 mM, NH_4HCO_3, pH 7.5), followed by incubation for 20 min at 37°C. The Cys residues present in the original disulfide bonds which did not undergo photolytic cleavage were subsequently converted to thiols and derivatized with DEM as follows: after derivatization of the photogenerated thiol residues by NEM, 80 µL of DTT were added to the insulin sample, and the sample was incubated for 20 min at 37°C, followed by the addition of 100 µL of DEM to derivatize the cysteine residues formed after DTT-reduction. This procedure ensured that all photolytically generated free thiols were derivatized with NEM and all remaining Cys residues were derivatized with DEM, i.e. labelled sufficiently different to be recognized by mass spectrometry analysis.

Digestion

The insulin solutions obtained after reduction and derivatization were incubated at 37°C for 3 h in the presence of 50 µg/mL Glu-C, i.e. an insulin/Glu-C ratio of 56:1.

Mass Spectrometry Analysis

Nano-Electrospray Ionization Time-Of-Flight Mass Spectrometry (ESI TOF MS) Analysis

ESI-MS spectra of undigested insulin and the peptide digests were acquired on a Q-TOF-2 (Micromass Ltd., Manchester, U.K.) hybrid mass spectrometer operated in the MS1 mode and acquiring data with the time-of-flight analyzer. ESI-MS spectra were also acquired on a SYNAPT-G2 (Waters Corp., Milford, MA). The Q-TOF-2 instrument was operated for maximum resolution with all lenses optimized on the $[M+2H]^{2+}$ ion from the cyclic peptide Gramicidin S. The cone voltage was 35 eV, Ar was admitted to the collision cell at a pressure that attenuates the beam to about 20% and the cell was operated at 12 eV (maximum transmission). Spectra were acquired at 16,129 Hz pusher frequency covering the mass range 350–2000 amu (amu = atomic mass unit) and accumulating data for 3 s per cycle. Time to mass calibration was made with CsI cluster ions acquired under the same conditions. The SYNAPT-G2 instrument was operated for maximum resolution with all lenses optimized on the $[M+2H]^{2+}$ ion from the $[Glu]^1$-Fibrinopeptide B. The cone voltage was 45 eV and Ar was admitted to the collision cell. The spectra were acquired using a mass range 300–3000 amu. The data were accumulated for 0.7 s per cycle.

MS/MS Analysis

The digested peptides were analyzed by means of an LTQ-FT hybrid linear quadrupole ion trap Fourier transform ion cyclotron resonance (FT-ICR) mass spectrometer (Thermo-Finnigan, Bremen, Germany) (43) and a SYNAPT-G2 (Waters Corp., Milford, MA). The MS/MS spectra were

analyzed with the software MassMatrix (44–47). MassMatrix was used to generate the theoretical fragment tables of the b and y ions of the different photoproducts involving the cysteine residues. The theoretical fragments were compared to the experimental MS/MS spectra to validate the structure of the photoproducts. The structures were validated only if the difference between the theoretical and the experimental m/z of the parent ion (and the fragment ions) was strictly below 0.1 Da.

Covalent H/D Exchange and Isotopic Correction

The deuterium content of peptide ions and their fragments was determined from the differences between the average mass of a covalently deuterated peptide and the average mass of the corresponding fully protonated peptide, according to our published protocol (22). The average masses were calculated from centroided isotopic distributions. The distribution of deuterium incorporation was obtained after isotopic correction by subtracting the isotope abundance distribution in the product formed during UV-irradiation in H_2O from the isotope abundance distribution of the same product generated in D_2O. This variation of the isotopic distribution between the experiments performed in deuterium oxide solution and water is given by the variation of the percent base peak intensity (%ΔBPI) (22).

Quantum Yield

The quantum yield for cystine photodegradation at 254 nm is 12-15% (48,49). In the presence of aromatic residues such as Phe and Tyr (insulin does not contain Trp), the quantum yield for disulfide bond cleavage is approximately 15-20% higher than during UV-irradiation of cystine alone (49).

The quantum yield (Φ) of photodegradation of solid insulin was measured at 253.7 nm with a band pass of 2 nm with an arc lamp (Model 68806; Oriel Instrument, Newport Corp., Irvine, CA) using an integrating sphere (Labsphere, Inc., North Sutton, NH), coupled to a monochromator (Model 77250; Oriel Instruments, Newport Corp., Irvine, CA). The device is described elsewhere (50). The solid insulin was placed on a quartz plate that had been designed to fit the integrating sphere. The lower intensity of incident light of the integrating sphere necessitated irradiation of up to 9 h. The irradiated and non-irradiated solids were dissolved in H_2O and analyzed by LC-MS (ESI-TOF-MS) to determine the number of moles of insulin lost during the photo-irradiation. Φ was calculated as follows: the number of moles of insulin lost during the irradiation, determined by LC-MS, was divided by the number of moles of photons used to photoirradiate the sample. According to this protocol, the quantum yield of insulin degradation was $\Phi(-\text{insulin}) = 7\%$. Quantum yields for reaction products were not determined due to the lack of synthetic standards for the photoproducts.

RESULTS

Sample Characterization

Determination of Zinc Content in Insulin

The crystallized and lyophilized bovine insulin samples were initially analyzed by polarized optical microscopy (Supplementary Material Fig. S1) and were consistent with crystalline and amorphous material, respectively. The crystallized insulin formed small rhombohedral-shaped particles that exhibited birefringence, while the lyophilized insulin formed thin irregular-shaped plates that did not birefringe. The crystalline content of both materials was further determined using the 2005 U.S. Pharmacopeia National Formulary (USP NF) method (34) reported in the insulin zinc suspension monograph, with the crystallized and lyophilized bovine insulin containing 92% and 0.1% crystalline material, respectively.

HPLC Method. The HPLC method was also used to measure the crystalline content of human insulin powder provided by Roche and of vacuum-dried preparations of solid insulin originally dissolved in either H_2O or D_2O. The insulin powder from Roche appeared to contain 46% crystalline material, while the vacuum-dried preparations contained 5% crystalline insulin according to the USP HPLC method (Fig. S2). The remaining 54% in the insulin powder supplied by Roche may consist of microparticles. In order to test the behavior of insulin microparticles in the USP HPLC method, we decided to prepare microcrystals according to published procedures (41). Analysis by scanning electron microscopy (SEM) revealed that the published procedure yielded insulin microparticles with diameters of ca. ≤ 3 μm for both insulin samples from Roche (Fig. S3, C) and Millipore (Fig. S3, D), respectively. These microparticles completely dissolve in the solvent system used in the USP method (buffered acetone, sodium acetate, sodium chloride, water) (34), indicating that the USP method may not be suited to differentiate between amorphous insulin and microparticles of insulin. On the other hand, SEM pictures of the commercial insulin powders from Roche (Fig. S3, A) and Millipore (Fig. S3, B) already demonstrate the presence of small crystals, potentially microcrystals, in the insulin which had not been subjected to the procedure for microcrystal preparation. We believe that this fraction may easily be dissolved by the solvents used for extraction of amorphous insulin (USP

method) and, therefore, should not be accounted for as "crystalline" insulin. The degree of crystallinity of the tested samples is summarized in Table 1.

^{13}C Solid-State NMR (SSNMR) Analysis of Solid Insulin. The ^{13}C-CP/MAS spectra of the two human insulin samples that were either supplied by Roche (46% crystalline, according to the USP HPLC procedure) or prepared in our laboratory (5% crystalline) are shown in Fig. 2 along, for comparison, with the crystalline (92% crystalline) and amorphous (0.1% crystalline) bovine insulin, respectively, prepared in our laboratory. There are no apparent differences between the spectra of the human insulin samples; the only observed differences (primarily at ~68 ppm and ~38 ppm) are likely due to noise. When comparing the bovine reference spectra, subtle differences are observed. One is that the line shape of the peak at ~175 ppm appears to consist of two poorly resolved peaks in the crystalline material with a small shoulder on the same peaks at ~180 ppm. Additionally, the peak at ~130 ppm also changes in line shape, and there is slightly better resolution of the peaks at ~137 and ~38 ppm in the crystalline insulin. When these features are compared with the human insulin spectra, it appears that the human insulin samples (Roche) are more amorphous in nature, which is consistent with the polarized light microscopy results (insulin from Roche; data not shown). It is important to note a slight difference in the amino acid sequences (the C-terminal Thr of the B chain of human insulin is replaced by Ala in bovine insulin), which may alter the spectra slightly but is not expected to significantly impact this interpretation. As part of the experimental setup, NMR relaxation properties of the human insulin samples were characterized; however, no significant differences were observed between the human insulin supplied by Roche and the solid human insulin prepared in our laboratory (see Fig. S4-S5).

Table I Degree of Crystallinity and Size of the Microparticles of the Different Insulin Samples

Insulin samples	Protocol	% Crystalline material	Size of microparticles
Roche Human insulin	none	46%[a]	NA
Roche Human insulin	vacuum dried	5%	NA
Roche Human insulin	microcrystallization	NA	≤ 3 μm
Millipore Human insulin	microcrystallization	NA	≤ 3 μm
Bovine insulin	freeze dried	92%	NA

[a] Based on the HPLC methods of the USP; the remaining 54% may be microparticles, which solubilize during the extraction with acetone buffer and cannot be distinguished from amorphous material by this method

Determination of the Zinc Content in Insulin

According to the protocol described in Determination of Zinc Content in Insulin, the molar ratio zinc:insulin in human insulin powder supplied by Roche is 7.2%. To validate this method, the zinc content in crystalline bovine insulin was measured using the same method. The molar ratio zinc:insulin in our crystalline bovine insulin preparation is 10.1%. This value is fairly consistent with the molar ratio of zinc:insulin used to prepare the crystalline structure (11.4%) (32,33). This method is therefore suited to determine the zinc content in the human insulin powder.

UV-Irradiation of Human Insulin

UV-irradiation of 2.8 mg of human insulin powder supplied by Roche and Millipore, respectively, yields two types of photoproducts, observed after Glu-C digestion: disulfide cleavage products, referred as to products I and II, and a dithiohemiacetal, referred to as product III (Table 2).

Products I and II represent peptides containing a Cys residue derivatized with NEM. Consistent with our derivatization scheme (see "Derivatization and Proteolytic Digestion of Photoirradiated Human Insulin"); these two Cys residues are, therefore, generated photolytically. The MS/MS fragmentation of products I and II (Fig. S6-S7) reveals most of the b and y fragments to identify their structures. These products are observed as traces. Their detection was possible only by use of the FT-ICR instrument, which displays a limit of detection below 10^{-15} moles. The injection of 4.8×10^{-9} mole of photo-irradiated insulin into the QTOF-2 instrument did not allow us to detect these photoproducts. Based on a limit of detection of the QTOF-2 instrument, calculated to ca. 5×10^{-12} moles, products I and II therefore represent less than 0.1% of the total mass of the irradiated insulin.

Product III represents the major photoproduct, for which MS/MS experiments suggest a dithiohemiacetal cross-link between Cys[B19] and Cys[A20], displayed in Fig. 3. The structure of this cross-link is fully rationalized by the observation of the y3-y6, b3, b6 and a5 fragments of the B-chain, and the y2, b2, and b3 fragments of the A-chain. In addition, the ion with m/z 636.74 would be consistent with a cleavage noted by δ, which provides further support for the formation of a dithiohemiacetal (the sulfur of Cys [B19] is cross-linked with the $^{\beta}$C of Cys[A20]) (Fig. 3). It is noteworthy that we observe product III also after UV-exposure of human insulin in aqueous solution (Fig. 4). In solution, product III is formed along with an isobaric product IV, corresponding to a crosslink between Cys[B19]

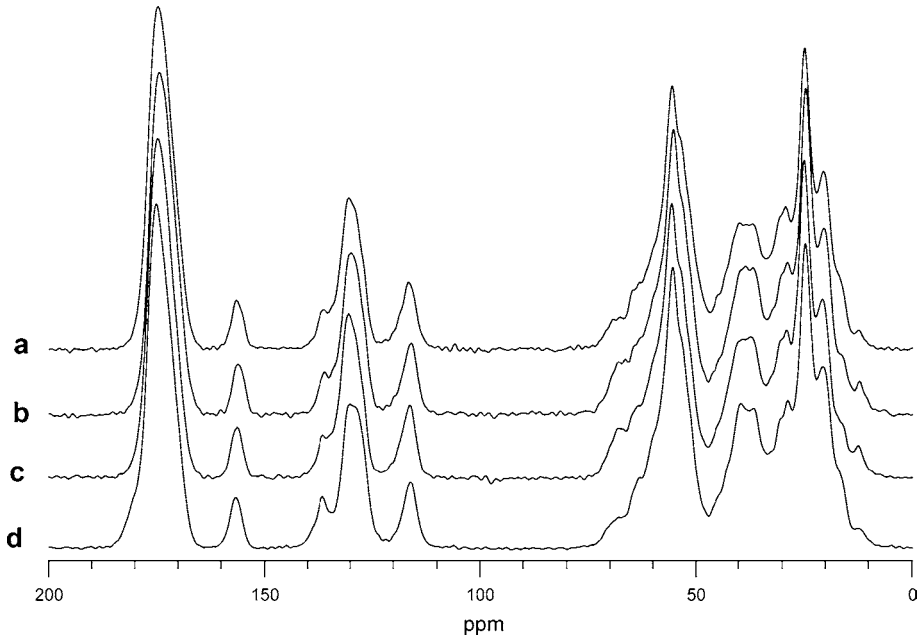

Fig. 2 ^{13}C-CP/MAS spectra of lyophilized and crystallized bovine insulin (**a**, **d**) and human insulin from Roche (**b**), and vacuum-dried human insulin from an aqueous solution (**c**).

Table 2 Structures of Photoproducts Obtained During Photo-Irradiation of Solid Insulin

Products	Structures
I	NH_2—F—V—N—Q—H—L–C(+NEM)–G—S—H—L—V—E—COOH
II	NH_2—A—L—Y—L—V–C(+NEM)–G—E—COOH
III	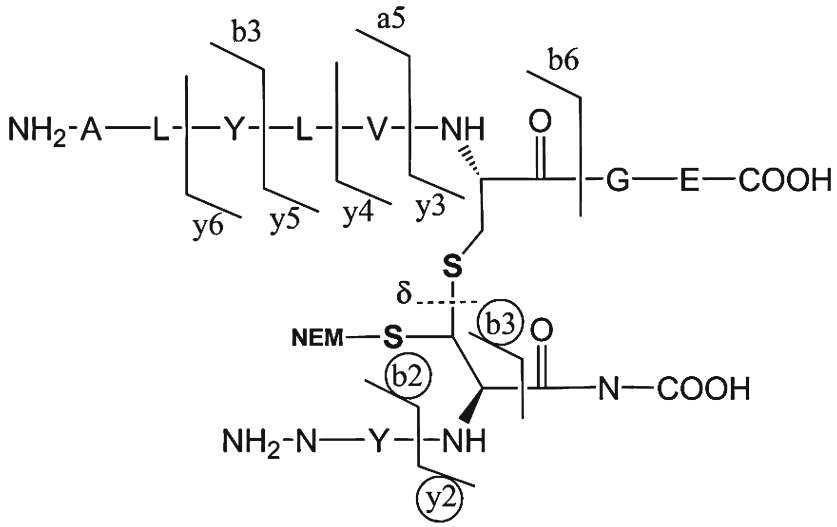

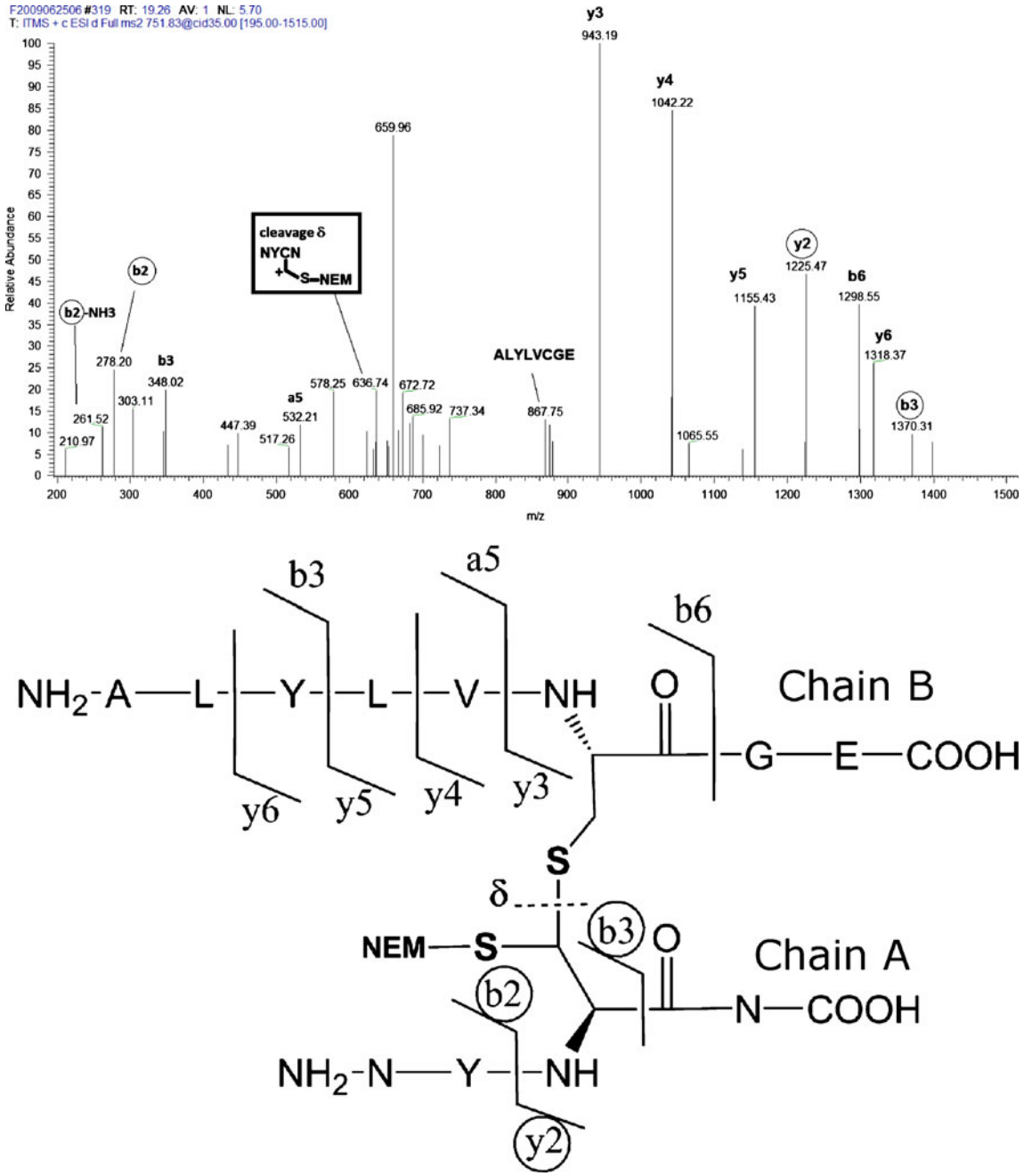

Fig. 3 CID mass spectrum obtained by means of a FT-MS mass spectrometer of NEM-derivatized fragments of insulin (m/z 751.8 $[M+H]^{+2}$) generated by UV-irradiation of solid-state insulin (powder supplied by Roche) and Glu-C digestion. The circled b and y fragments are obtained after MS/MS of the chain A.

and Tyr[A19] (22). Most of the b and y fragment ions characteristic of III and IV are identical. However, the presence of some specific b2 and y2 fragment ions, albeit in low yields (Fig. 4, squared ions), provide evidence for the formation of a crosslink between Cys[B19] and Tyr[A19] in solution. Initially, we had reported product IV as the only crosslink formed in solution (22), but the higher quality of our MS/MS data in the current paper together with our recent mechanistic understanding of dithiohemiacetal formation in solution (18,20) now permits us to identify the formation of both III and IV in solution. In the solid, the yield of product III was sufficient for detection by the QTOF-2 instrument. The number of counts allows for estimating the content of product III as 0.7% of the total mass of the photo-irradiated insulin, corresponding to 3.4 μM concentration of product III for 482 μM of insulin photo-irradiated and obtained after reconstitution of 2.8 mg/mL of solid insulin in 400 μL of H_2O (Table 3). In comparison, in solution, the yield of

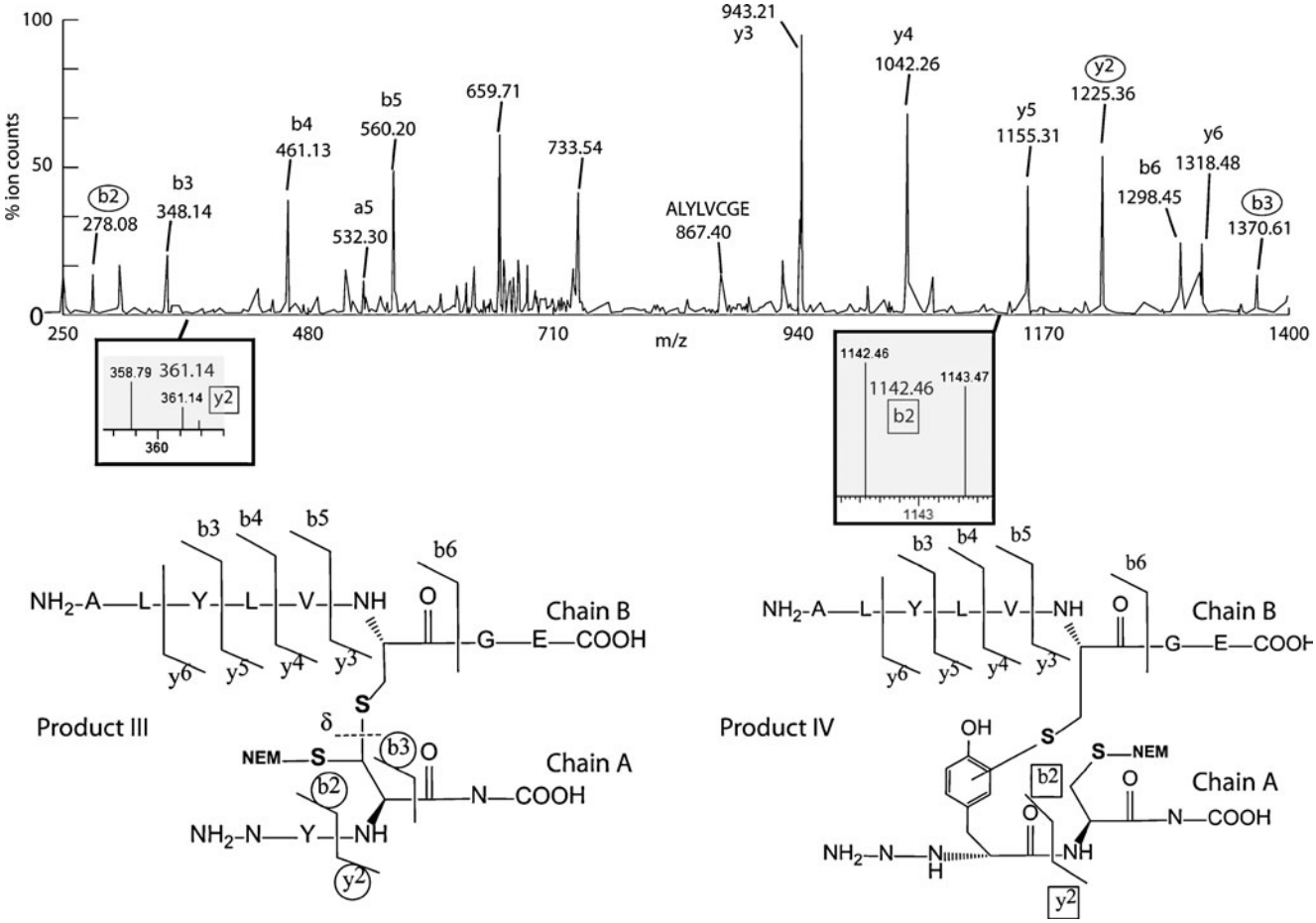

Fig. 4 CID mass spectrum obtained by means of a FT-MS mass spectrometer of NEM-derivatized fragments of insulin (m/z 751.8 $[M+H]^{+2}$) generated by UV-irradiation of aqueous solution of human insulin (Roche) and Glu-C digestion. The circled b and y fragments are obtained after MS/MS of chain A from product III. The squared b and y fragments are obtained after MS/MS of chain A from product IV.

product III (along with IV) is estimated to be ca. 40-fold higher. Notably, the MS/MS spectra of product III were reproduced on two different mass spectrometers, the FT-ICR (Fig. 3) and the SYNAPT-G2 (Fig. 5).

UV-Irradiation of Amorphous Human Insulin

Insulin (2.8 mg) was diluted in 1 mL of H_2O and D_2O, followed by drying under vacuum in a SpeedVac. This procedure formed insulin that was only 5% crystalline. The photoirradiation of this sample generated products I, II and III in comparable yields as the UV-exposure of the powder of human insulin supplied by Roche ("UV-Irradiation of Human Insulin"). Photoirradiation of dried insulin was established to examine the feasibility of an intramolecular reversible hydrogen transfer between $CysS^{\bullet}$ and $^{\alpha}C$-H in solid state (see Scheme 1). Such intramolecular hydrogen transfer was demonstrated for human insulin in aqueous solution (22).

Product III was the major photoproduct detected after photo irradiation of the amorphous insulin obtained upon drying from aqueous (H_2O and D_2O) solutions of human insulin. The dissolution of insulin into D_2O prior to drying is expected to produce residual D_2O (instead of H_2O) in the dried sample (in addition to H/D exchange at exchangeable sites such as original NH, OH, and SH bonds). After photo irradiation and resolubilization of photoirradiated insulin in H_2O, product III contained no covalently bound deuterium, suggesting that thiyl radical-mediated covalent H/D exchange cannot compete with the formation of product III in solid insulin.

Table 3 Yields of Photoproducts Relative to Total Insulin Content

Solid human insulin	Products I and II	Product III
Crystalline insulin from Roche	<0.1%	<0.7%
Amorphous insulin	<0.1%	<0.7%
Microcrystalline insulin from Millipore	<0.1%	<0.07%

UV-Irradiation of Microparticulate Human Insulin

Microparticles prepared from Millipore insulin (2.8 mg) were irradiated at 253.7 nm. The UV-irradiation of the

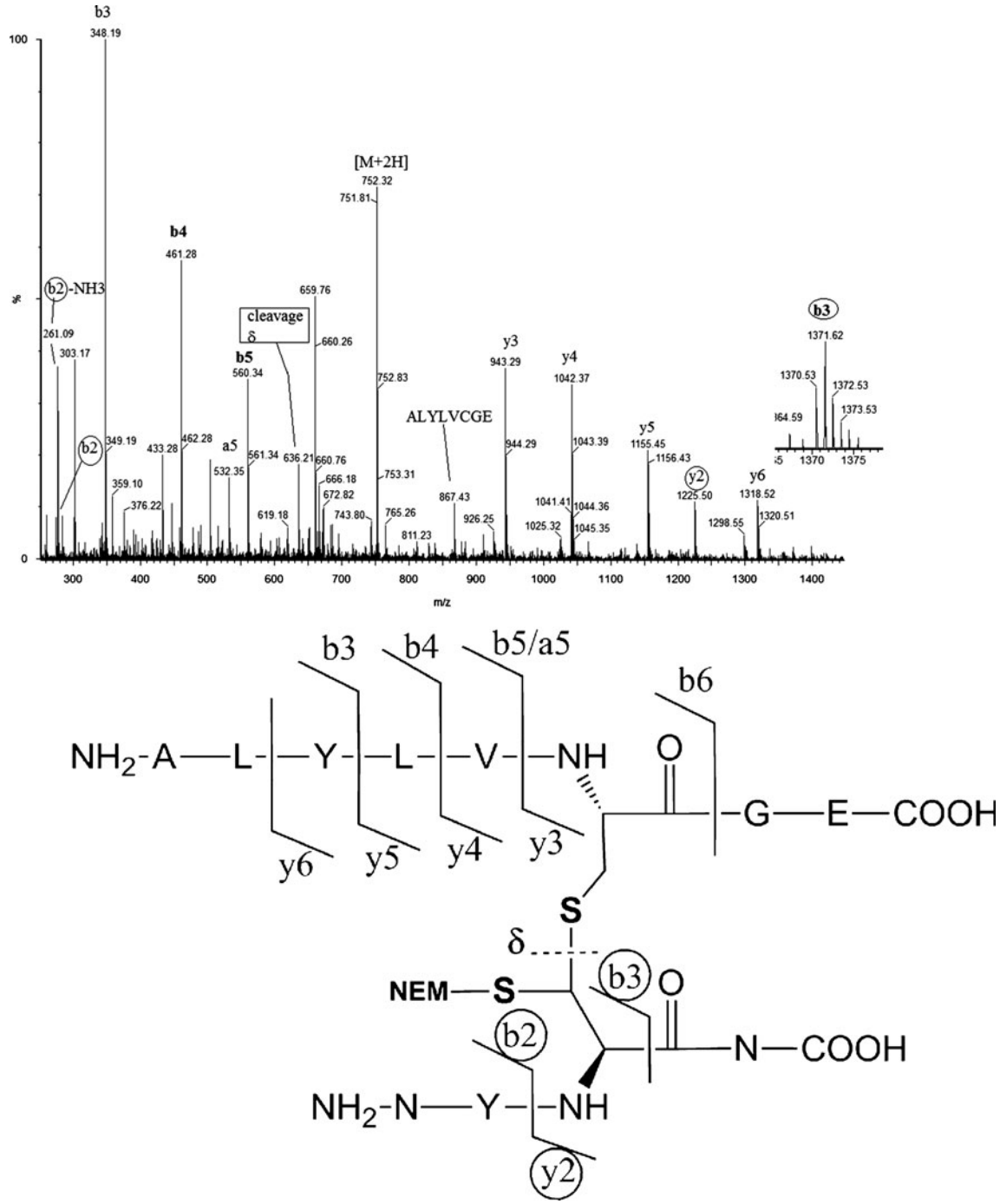

Fig. 5 CID mass spectrum obtained by means of a SYNAPT-G2 mass spectrometer of NEM-derivatized fragments of human insulin (m/z 751.8 $[M+H]^{+2}$) generated by UV-irradiation of solid insulin powder (supplied by Millipore) and Glu-C digestion. The circled b and y fragments are obtained after MS/MS of chain A.

crystalline insulin powder and of the microparticles from Millipore insulin results in the formation of product III. However, the mass spectrometry results reveal that product III is ca. 10 times less abundant after UV-irradiation of our microparticle preparation than after UV exposure of the original crystalline powder (Table 3).

DISCUSSION

Nature of the Photoproducts

Three photoproducts are observed after 253.7 nm photolysis of insulin in the solid state (Table 2). Products

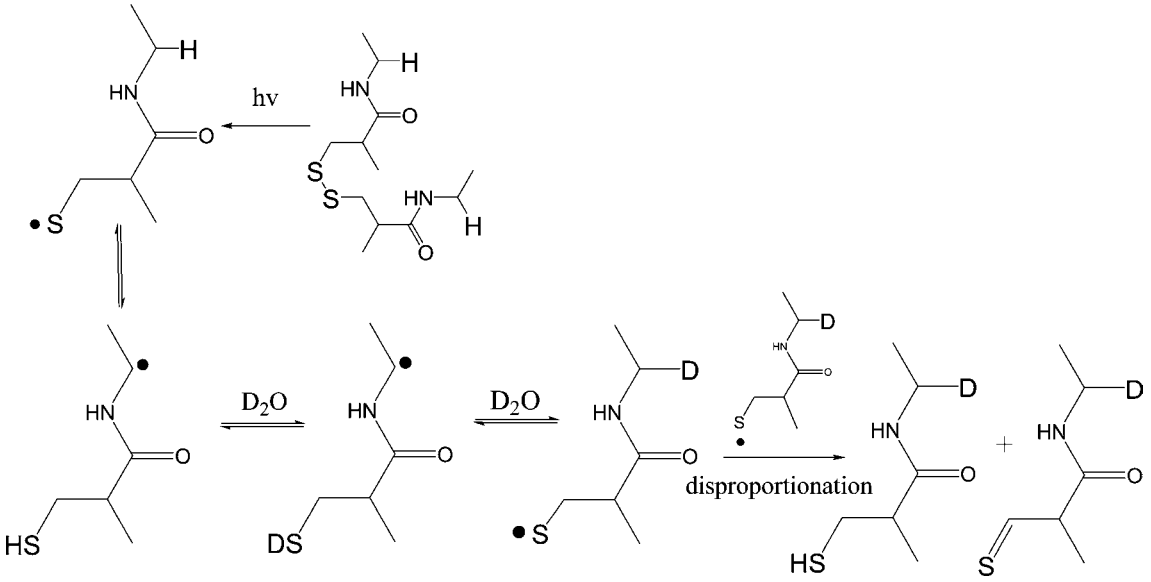

Scheme 1 Reaction scheme for covalent H/D exchange. The intramolecular H-transfer occurs between the thiyl radical group of the cysteine residue and $^{\alpha}$C-H.

I and II contain reduced Cys at positions Cys[B7] and Cys [B19] (derivatized with NEM), while product III requires Cys thiol formation according to the reactions described in Scheme 2. Mechanistic details on the formation of analogous products have been characterized for the solution photochemistry of disulfide-containing model peptides (18,20). In the solid state, the yields from insulin are ca. 40-fold lower compared to photo irradiation in aqueous solution. Photoproduct III indicates photo-induced rearrangement of the native C-terminal disulfide bond (Scheme 2). We are not able to clearly identify such a product in the N-terminal region of insulin because of the lack of a digestion site between Cys[A6] and Cys [A11], which makes the structure of the product highly complex for analysis by MS/MS sequencing. Product III contains a dithiohemiacetal similar to the dithiohemiacetal structures identified after the photoirradiation of model peptides containing intrachain disulfide bonds (20). For the latter peptides, we have characterized subsequent reactions which convert dithiohemiacetal to thioethers (prolonged UV exposure) or vinyl-sulfides and trisulfides (exposure to 40°C for 8 h). Hence, dithiohemiacetal structures in insulin must be considered as potential origin for secondary products, which can form during storage but potentially also after administration of the protein. In this regard it is important to note that a thioether variant of hGH had a significantly reduced affinity to its receptor (23), indicating that the mere removal of a sulfur atom from a disulfide bond can have significant conformational consequences.

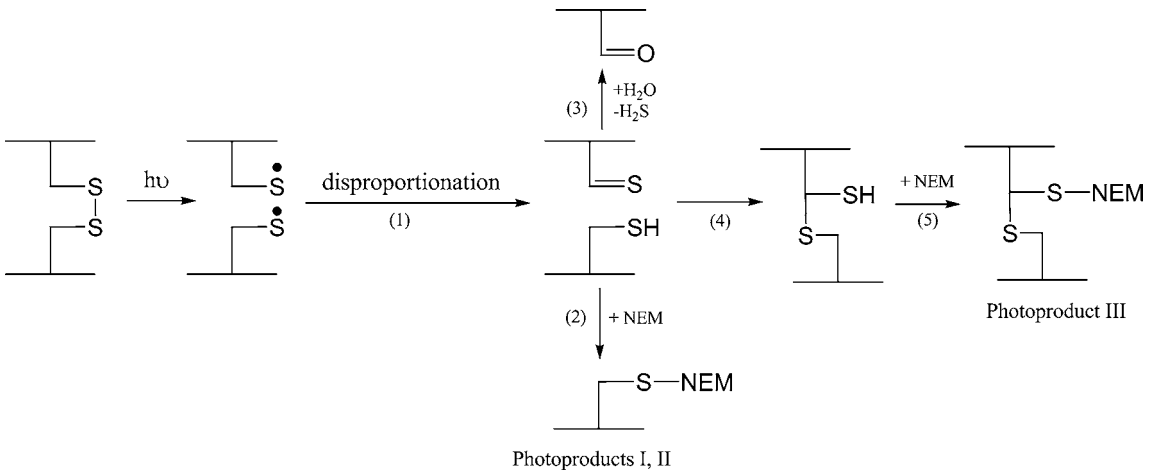

Scheme 2 Reaction scheme leading to the formation of the photoproducts generated after photolysis at 253.7 nm of solid state insulin.

Examination of the Secondary Structure

The secondary structure of Millipore insulin is not damaged after UV-irradiation of the solid. The UV-exposure of insulin in solution leads to a loss of helicity (Fig. S8).

The Absence of Covalent Deuterium Incorporation

A reversible H-atom transfer between $CysS^{\bullet}$ and $^{\alpha}C$-H bonds (Scheme 1) was not observed in solid insulin (contrary to insulin in solution, (22)). We believe that this is likely the result of conformational restriction. The recombination process of the thiyl radicals ($CysS^{\bullet}$[B19] and $CysS^{\bullet}$[A20]) or the disproportionation of these thiyl radicals into thioaldehyde and thiol, followed by the formation of product III, outcompetes the reversible intramolecular H-atom transfer. The proximity in space of the thioaldehyde and thiol species allows the formation of III even in the solid state (Scheme 2, reaction 4).

Effect of Insulin Physical Form

Significant differences were observed in the physical form of the human insulin that was provided by Roche and the vacuum-dried samples, with materials containing ~50% crystalline (and possibly 50% microcrystals/microparticles) and ~5% crystalline insulin, respectively. Despite previous observations of crystalline and amorphous insulin having significantly different stabilities (31), the physical form of the insulin appears to have no observed effect on the formation of dithiohemiacetal under photo-irradiation conditions. Product III is formed during the UV-irradiation of i) the original powders from Roche and Millipore, ii) amorphous insulin prepared from the Roche powder, and iii) microparticles prepared from the Millipore insulin powder (Table 3). However, especially the microparticulate sample showed significantly reduced yields. We have currently no explanations for this observation.

CONCLUSION

The development of proteins as a class of potent therapeutic drugs has intensified over the last decade. In parallel, the understanding of chemical and physical degradation pathways of proteins has received increasing interest. Because the degradation of proteins may generate products that are potentially immunogenic, it is mandatory to screen how different parameters such as temperature, light-exposure, pressure, humidity, and pH may affect the stability of proteins during production, purification and storage. Though the effects of temperature, pressure, and pH are routinely investigated to characterize the stability of proteins, the effect of light is frequently not considered. However, UV exposure might induce structural and eventually functional alterations of proteins. The use of UV light ($\lambda < 280$ nm) during purification, analysis and sterilization (51) might be critical to the initiation of degradation in cystine-containing proteins. Whereas the formulation of solid insulin significantly diminishes the formation of light-induced products compared to solutions, the rearrangement of a disulfide bond into dithiohemiacetal cannot be avoided. Future experiments will be undertaken to understand the role of a dithiohemiacetal, if any, in aggregation and/or immunogenicity that may occur during photolytic or any other degradation processes of insulin.

ACKNOWLEDGMENTS & DISCLOSURES

We are grateful to Amgen Inc. for financial support, and thank Dr. Nadya Galeva for operating the FT-ICR instrument.

REFERENCES

1. Krejsa C, Rogge M, Sadee W. Protein therapeutics: new applications for pharmacogenetics. Nat Rev Drug Discov. 2006;5:507–21.
2. Cornell M, Chou DK, Murphy BM, Payne RW, Katayama DS. Stability of protein pharmaceuticals: an update. Pharm Res. 2010;27:544–75.
3. Manning MC, Patel K, Borchardt RT. Stability of protein pharmaceuticals. Pharm Res. 1989;6:903–18.
4. Hongo-Hirasaki T, Yamaguchi K, Yanagida K, Okuyama K. Removal of small viruses (parvovirus) from IgG solution by virus removal filter Planova 20 N. J Membr Sci. 2006;278:3–9.
5. Phillips M, Cormier J, Ferrence J, Dowd C, Kiss R, Lutz H, *et al.* Performance of a membrane adsorber for trace impurity removal in biotechnology manufacturing. J Chromatogr A. 2005;1078:74–82.
6. Kerwin BA, Remmele RL. Protect from light: photodegradation and protein biologics. J Pharm Sci. 2007;96:1468–79.
7. Purdie JW, Gillis HA, Klassen NV. The pulse radiolysis of penicillamine and penicillamine disulfide in aqueous solution. Can J Chem. 1973;51:3132–42.
8. Hoffman MZ, Hayon E. One-electron reduction of the disulfide linkage in aqueous solution. Formation, protonation, and decay kinetics of the RSSR radical. J Am Chem Soc. 1972;94:7950–7.
9. Yee CS, Chang MC, Ge J, Nocera DG, Stubbe J. 2,3-difluorotyrosine at position 356 of ribonucleotide reductase R2: a probe of long-range proton-coupled electron transfer. J Am Chem Soc. 2003;125:10506–7.
10. Bennati M, Robblee JH, Mugnaini V, Stubbe J, Freed JH, Borbat P. EPR distance measurements support a model for long-range radical initiation in E. coli ribonucleotide reductase. J Am Chem Soc. 2005;127:15014–5.
11. Rigby SE, Hynson RM, Ramsay RR, Munro AW, Scrutton NS. A stable tyrosyl radical in monoamine oxidase A. J Biol Chem. 2005;280:4627–31.
12. Zhang H, Xu Y, Joseph J, Kalyanaraman B. Intramolecular electron transfer between tyrosyl radical and cysteine residue inhibits tyrosine nitration and induces thiyl radical formation in model peptides treated with myeloperoxidase, H2O2, and NO2-: EPR SPIN trapping studies. J Biol Chem. 2005;280:40684–98.

13. Wang M, Gao J, Muller P, Giese B. Electron transfer in peptides with cysteine and methionine as relay amino acids. Angew Chem Int Ed Engl. 2009;48:4232–4.
14. Mozziconacci O, Mirkowski J, Rusconi F, Pernot P, Bobrowski K, Houee-Levin C. Superoxide radical anions protect enkephalin from oxidation if the amine group is blocked. Free Radic Biol Med. 2007;43:229–40.
15. Backes G, Sahlin M, Sjoberg BM, Loehr TM, Sanders-Loehr J. Resonance Raman spectroscopy of ribonucleotide reductase. Evidence for a deprotonated tyrosyl radical and photochemistry of the binuclear iron center. Biochemistry. 1989;28:1923–9.
16. Hossain MA, Thomas F, Hamman S, Saint-Aman E, Boturyn D, Dumy P, *et al.* Cyclodecapeptides to mimic the radical site of tyrosyl-containing proteins. J Pept Sci. 2006;12:612–9.
17. Naumov S, Schöneich C. Intramolecular addition of cysteine thiyl radical to phenylalanine and tyrosine in model peptides, Phe (CysS) and Tyr(CysS): a computational study. J Phys Chem A. 2009;113:3560–5.
18. Mozziconacci O, Kerwin BA, Schöneich C. The exposure of a monoclonal antibody, IgG1, to UV-light leads to protein dithiohemiacetal and thioether cross-links. Chem Res Toxicol. 2010;23:1310–2.
19. Mozziconacci O, Kerwin BA, Schöneich C. Reversible hydrogen transfer between cysteine thiyl radical and glycine and alanine in model peptides: covalent H/D exchange, radical-radical reactions, and L- to D-Ala conversion. J Phys Chem B. 2010;114:6751–62.
20. Mozziconacci O, Kerwin B, Schöneich C. Photolysis of an intrachain peptide disulfide bond: primary and secondary processes, formation of H_2S, and hydrogen transfer reactions. J Phys Chem B. 2010;114:3668–88.
21. Mozziconacci O, Sharov V, Williams TD, Kerwin BA, Schöneich C. Peptide cysteine thiyl radicals abstract hydrogen atoms from surrounding amino acids: the photolysis of a cystine containing model peptide. J Phys Chem B. 2008;112:9250–7.
22. Mozziconacci O, Williams T, Kerwin B, Schöneich C. Reversible intramolecular hydrogen transfer between protein cysteine thiyl radicals and αC-H bonds in insulin: control of selectivity by secondary structure. J Phys Chem B. 2008;112:15921–32.
23. Lispi M, Datola A, Bierau H, Ceccarelli D, Crisci C, Minari K, *et al.* Heterogeneity of commercial recombinant human growth hormone (r-hGH) preparations containing a thioether variant. J Pharm Sci. 2009;98:4511–24.
24. Datola A, Richert S, Bierau H, Agugiaro D, Izzo A, Rossi M, *et al.* Characterisation of a novel growth hormone variant comprising a thioether link between Cys182 and Cys189. Chem Med Chem. 2007;2:1181–9.
25. Scheffer J. Geometric requirements for intramolecular photochemical hydrogen atom abstraction: studies based on a combination of solid state chemistry and x-ray crystallography., Desiraju, G. R., Amsterdam, 1987.
26. Mc Bride JM. The role of local stress in solid-state radical reactions. Acc Chem Res. 1983;16:304–12.
27. Jameel F, Tchessalov S, Bjornson E, Lu X, Besman M, Pikal M. Development of freeze-dried biosynthetic Factor VIII: I. A case study in the optimization of formulation. Pharm Dev Technol. 2009;14:687–97.
28. Patel SM, Pikal M. Process analytical technologies (PAT) in freeze-drying of parenteral products. Pharm Dev Technol. 2009;14:567–87.
29. Miller BL, Hageman MJ, Thamann TJ, Barr n LB, Schöneich C. Solid-state photodegradation of bovine somatotropin (bovine growth hormone): evidence for tryptophan-mediated photooxidation of disulfide bonds. J Pharm Sci. 2003;92:1698–709.
30. McLaren AD, Shugar D, editors. Photochemistry of proteins and nucleic acids. Oxford: Pergamon; 1964.
31. Pikal MJ, Rigsbee DR. The stability of insulin in crystalline and amorphous solids: observation of greater stability for the amorphous form. Pharm Res. 1997;14:1379–87.
32. Schlichtkrull J. Insulin Crystals II. Shape of rhombohedral zinc-insulin crystals in relation to species and crystallization media. Acta Chem Scand. 1956;10:1459–64.
33. Schlichtkrull J. Insulin Crystals III. Determination of the rhombohedral zinc-insulin unit-cell by combined microscopical and chemical exminations. Acta Chem Scand. 1957;11:291–8.
34. Bailey MM, Gorman EM, Munson EJ, Berkland C. Pure insulin nanoparticle agglomerates for pulmonary delivery. Langmuir. 2008;24:13614–20.
35. Crow JP, Sampson JB, Zhuang Y, Thompson JA, Beckman JS. Decreased zinc affinity of amyotrophic lateral sclerosis-associated superoxide dismutase mutants leads to enhanced catalysis of tyrosine nitration by peroxynitrite. J Neurochem. 1997;69:1936–44.
36. Metz G, Wu X, Smith S. Ramped-amplitude cross polarization in magic-angle-spinning NMR. J Magn Reson Ser A. 1994;110:219–27.
37. Stejskal E, Schaefer J, Waugh J. Magic-angle spinning and polarization transfer in proton-enhanced NMR. J Magn Reson. 1977;28:105–12.
38. Fung B, Khitrin A, Ermolaev K. An improved broadband decoupling sequence for liquid crystals and solids. J Magn Reson. 2000;142:97–101.
39. Barich D, Gorman E, Zell M, Munson E. 3-Methylglutaric acid as a 13C solid-state NMR standard. Solid State Nucl Mag. 2006;30:125–9.
40. Kwon JH, Kim CW. A novel insulin microcrystals preparation using a seed zone method. Cryst Growth. 2004;263:536–43.
41. Kwon JH, Lee BH, Lee JJ, Kim CW. Insulin microcrystal suspension as a long-acting formulation for pulmonary delivery. Eur J Pharm Sci. 2004;22:107–16.
42. Rahn RO, Stefan MI, Bolton JR, Goren E, Shaw PS, Lykke KR. Quantum yield of the iodide-iodate chemical actinometer: dependence on wavelength and concentrations. Photochem Photobiol. 2003;78:146–52.
43. Ikehata K, Duzhak TG, Galeva NA, Ji T, Koen YM, Hanzlik RP. Protein targets of reactive metabolites of thiobenzamide in rat liver *in vivo*. Chem Res Toxicol. 2008;21:1432–42.
44. Xu H, Freitas MA. MassMatrix: a database search program for rapid characterization of proteins and peptides from tandem mass spectrometry data. Proteomics. 2009;9:1548–55.
45. Xu H, Freitas MA. A mass accuracy sensitive probability based scoring algorithm for database searching of tandem mass spectrometry data. BMC Bioinformatics. 2007;8:133.
46. Xu H, Yang L, Freitas MA. A robust linear regression based algorithm for automated evaluation of peptide identifications from shotgun proteomics by use of reversed-phase liquid chromatography retention time. BMC Bioinformatics. 2008;9:347.
47. Xu H, Zhang L, Freitas MA. Identification and characterization of disulfide bonds in proteins and peptides from tandem MS data by use of the MassMatrix MS/MS search engine. J Proteome Res. 2008;7:138–44.
48. Asquith RS, Hirst L. The photochemical degradation of cystine in aqueous solution in the presence of air. Biochim Biophys Acta. 1969;184:345–57.
49. Dose K. The photolysis of free cystine in the presence of aromatic amino acids. Photochem Photobiol. 1968;8:331–5.
50. Barrón LB, Waterman KC, Filipiak P, Hug GL, Nauser T, Schöneich C. Mechanism and Kinetics of Photoisomerization of a Cyclic Disulfide, trans-4,5-Dihydroxy-1,2-dithiacyclohexane. J Phys Chem A. 2004;108:2247–55.
51. Lorenz CM, Wolk BM, Quan CP, Alcala EW, Eng M, McDonald DJ, *et al.* The effect of low intensity ultraviolet-C light on monoclonal antibodies. Biotechnol Prog. 2009;25:476–82.